EasyChair Preprint

№ 7782

The Phenomenon of Extinction of Timber - Experiments and Theory

V.M Jaganathan, S Varunkumar, R. Varun Kumar, Juan Cuevas and Cristian Maluk

April 12, 2022

AOSFST 2021 – 12th Asia-Oceania Symposium on Fire Science and Technology
The University of Queensland, Brisbane, Australia, 7-9 December 2021

Full paper title: The phenomenon of extinction of timber – Experiments and theory

1st Author
First Name: Jaganathan
Last Name: V M
Ttitle, Affiliation: Department of Energy and Environment, National Institute of Technology Tiruchirappalli, Tamil Nadu, India
ORCID: https://orcid.org/0000-0001-6680-8342

2nd Author
First Name: Varunkumar
Last Name: S
Ttitle, Affiliation: Department of Mechanical Engineering, IIT Madras, Tamil Nadu, India
ORCID: https://orcid.org/0000-0002-8765-1257

3rd Author
First Name: R
Last Name: Varun Kumar
Ttitle, Affiliation: Department of Energy and Environment, National Institute of Technology Tiruchirappalli, Tamil Nadu, India

4th Author
First Name: Juan
Last Name: Cuevas
Ttitle, Affiliation: School of Civil Engineering, The University of Queensland, Brisbane, Australia
ORCID: https://orcid.org/0000-0002-1504-5530

5th Author
First Name: Cristian
Last Name: Maluk
Ttitle, Affiliation: School of Civil Engineering, The University of Queensland, Brisbane, Australia
ORCID: https://orcid.org/0000-0000-0000-0000

https://doi.org/XXX

AOSFST 2021 – 12th Asia-Oceania Symposium on Fire Science and Technology
The University of Queensland, Brisbane, Australia, 7-9 December 2021

THE PHENOMENON OF EXTINCTION OF TIMBER - EXPERIMENTS AND THEORY

Jaganathan V M[1], Varunkumar S[2], R Varun Kumar[3], Juan Cuevas[4], Cristian Maluk[5]

ABSTRACT

The phenomenon of self-extinction plays a vital role in predicting the structural integrity of timber structures in mid-and high-rise constructions when exposed to fire. In the present study, the flame propagation, spatial temperature variations with time, and criteria for self-extinction of a Cross Laminated Timber (CLT) block subjected to fire are predicted using the "Unified ignition Devolatilization" (UID) model. The effects of incident heat flux, oxygen concentration on flame propagation, and self-extinction were studied. The mass loss rate (MLR) for different operating conditions were predicted and validated with the experiments done at controlled atmospheres. The model is shown to predict the overall behavior accurately with the predictions of MLR close to the experimental values.

Keywords: self-extinction, CLT, devolatilization, flame propagation, UID model.

1 INTRODUCTION

1.1 Background

The use of Cross Laminated Timber (CLT) in mid and high-rise construction is widespread. Understanding the behavior of CLT under fire is critical to evolving model-based safety strategies. Towards this, the ignition, burning and possible self-extinction of CLT blocks under a variety of conditions have been studied using a combination of experimental and theoretical approaches. Details of these studies are presented here. To account for the varying heat flux and oxygen concentrations a block a CLT could be subjected to in an actual fire, experiments covering a range of incident heat flux and oxygen concentrations have been studied. The cases for which data is reported here are summarized in Table 1.

Table 1. Experimental conditions presented in the current study

S.No	Oxidizer	Ignition heat flux * (kW/m^2)	Heat flux after Ignition * (kW/m^2)	Remarks
1	Air	50	30	Extinction observed
2	Air	50	40	No Extinction

* Ignition heat flux is maintained for a time period of 1200 seconds from the start of experiment.

* After 1200 seconds, heat flux is varied to study the effect of extinction till 3600 seconds.

[1] Department of Energy and Environment, National Institute of Technology Tiruchirappalli, Tamil Nadu, India
e-mail: vmjagan@ntt.edu, ORCID: https://orcid.org/0000-0001-6680-8342

[2] Department of Mechanical Engineering, IIT Madras, Tamil Nadu, India
e-mail: varuns@iitm.ac.in, ORCID: https://orcid.org/0000-0002-8765-1257

[3] Department of Energy and Environment, National Institute of Technology Tiruchirappalli, Tamil Nadu, India
e-mail: 202319011@nitt.edu,

[4] Department of Fire Protection Engineering, Worcester Polytechnic Institute, Worcester, U.S.
e-mail: jcuevas@wpi.edu, ORCID: https://orcid.org/0000-0002-1504-5530

[5] School of Civil Engineering, The University of Queensland, Brisbane, Australia
e-mail: c.maluk@uq.edu.au, ORCID: https://orcid.org/0000-xxxx-xxxx-xxxx

https://doi.org/XXX

There are a number of studies (predominantly experimental) on the ignition, burning and extinction of CLT blocks [1-18]. The unique feature of the current study is the development of a modeling framework for analysis and prediction of behavior of CLT under fire conditions. The modelling framework reported here is based on the 'Unified Ignition and Devolatilization model' (referred to as UID model from hereon). The principal feature of the UID model that sets it apart from the other prevalent approaches is the assumption that all the processes that a biomass based solid fuel (CLT block in the current case) undergoes are transport controlled. While this may appear like a drastic simplification, extensive use of this approach to model phenomena including, combustion of single particles (of sizes from as small as a few tens of micron to a few cm), flame propagation in packed beds and stability of particle laden flames in MILD burners, have proved its validity [19-23]. The primary reason for the success of this approach is the following - under actual combustion and fire like conditions, the heating rate that a material is subject to is in the order of 1000 - 10000 K/min; therefore, chemical reaction rates are high enough for the zones of chemical decomposition to be confined to layers which are at least an order of magnitude thinner compared to non-reactive zone. Hence, zones with chemical reactions are essentially interfaces separating fresh material from char. Under such conditions, the rate controlling step is the heat up time in non-reactive zones and therefore the assumption of transport control is accurate. The key advantage of the UID approach is that the transport controlled models enjoy greater predictive capability compared to models requiring kinetic parameters as inputs.

1.2 The Influence of Oxygen Concentrations

In the area of timber combustion research, fire research, and the use of timber as fuel, the effect of oxygen concentrations in the atmosphere plays a significant role in the burning behaviour of timber [9]. By reducing the oxygen concentration in the atmosphere, it is found that the time to ignition increases [9]. Furthermore, a decrease in ambient oxygen concentration will reduce the flame temperature as soon as the ignition is achieved. An obvious direct effect of this is that thermal feedback from the flame to the solid's surface is decreased. When the flame temperature drops to 1500K, extinction probability is high [14]. It has been reported that a decrease in the sample's MLR when tested with deficit oxygen concentrations in the atmosphere [11]. Also, it is found that a deficit in the oxygen concentration will lead to lower char oxidation rates [10,13]; this dependence of oxygen parameter has a weak one over the pyrolysis front and a strong influence over char oxidation. Therefore, for low O_2 concentrations, the thickness of the char layer will increase [9]. This leads to less heat at the surface of the timber and is sent to the pyrolysis front. The charring rate is decreased; this latter will unavoidably affect the circumstances that lead to the self-extinction of cross-laminated timber.

2 EXPERIMENTAL APPROACH

2.1 Experimental setup

A series of experiments were conducted using FM Global's Fire Propagation Apparatus (FPA). A simplified schematic of the FPA is presented in Fig.1. In the test section of the FPA, the sample is exposed to incident heat on a single, horizontally-oriented surface through a set of four infrared heaters that deliver heat fluxes of up to 100 kW/m^2. Before every test, the heat incident heat flux from the lamps was characterised using a Schmidt-Boelter-type heat flux gage. A low-emissivity jet pilot flame located 1 cm above the exposed face of the sample was used to trigger ignition. To specify the atmosphere under which the samples were tested, three mass-flow controllers (MFC) were used to adjust the flows of air, N_2 and O_2 that are delivered to the combustion chamber. A quartz tube of 160mm ID was used to confine the atmosphere under which the samples were tested.

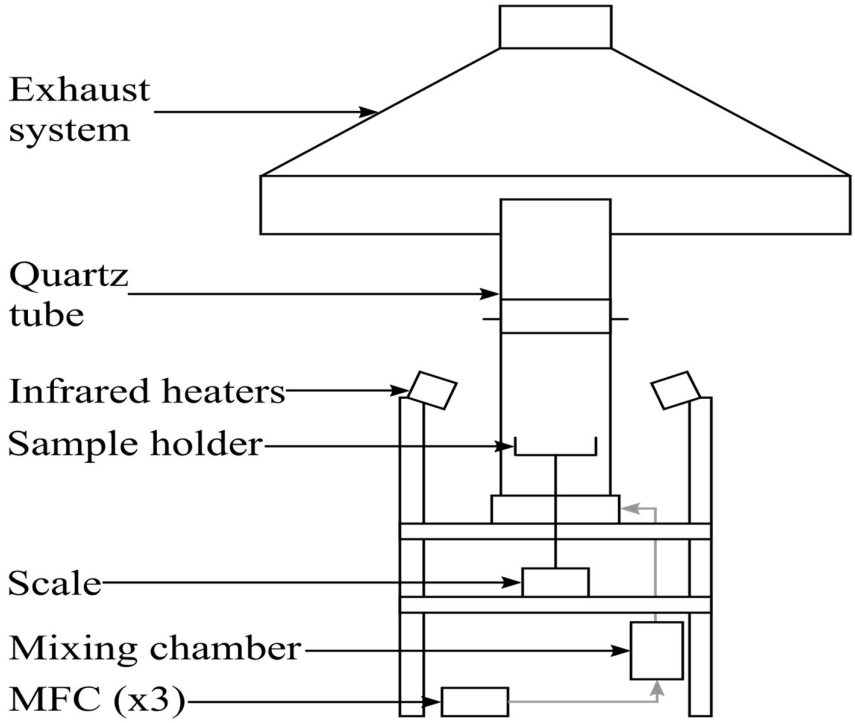

Fig.1 Schematic of the FPA

Within the scope of this study, two types of tests were conducted. One aimed at measuring the mass loss of the sample, and another aimed at capturing the evolution of the temperature within it. For the first type of study, the sample is positioned on top of a sample holder connected to a load cell (±3 g accuracy, 1 Hz sampling rate) that registers the change in mass for the duration of the test. For the second type of experiment, 12 type-K thermocouples were embedded at different depths from the exposed surface within the sample. The readings from the thermocouples were collected at a frequency of 4 Hz.

2.2 Conditions studied and sample preparation

The experiments were conducted under atmospheres with 17, 19, and 21% oxygen concentration. For all experiments, the flow of oxidizer towards the sample was kept at a constant 200 slpm. Data pertaining to air cases are presented and described in this study. However, the model described in this paper is applicable for other oxygen cases as well.

Based on the work of Emberley et al. [24] the experiments comprised two sequential stages. First, the samples were exposed to a constant incident heat flux of 50 kW/m^2, until a thermal steady-state was reached. Once steady-state is reached, the incident heat flux was decreased. If self-extinction occurred, the incident heat flux, time of extinction, and mass-loss rate at extinction were recorded. As a result of this methodology, external incident heat fluxes in the range of 30-50 kW/m^2 were used. For all of these thermal exposures, the incident heat flux over any point of the exposed surface was found to deviate no more than 5% from the mean value.

The test samples were made of commercially-available 5-ply Radiata Pine with a cross-section of 90x90 mm^2 (that matches with the dimensions of the exposed face of the sample) and a thickness of 150 mm. The sides of the sample were protected with a layer of ceramic insulation (9mm thick) and an outer layer of aluminium foil to ensure the heating of only one exposed face. More details on the experimental setup and conditions can be obtained from [18].

3 NUMERICAL MODELLING

To understand the single-particle burning of timber, a modified 'Unified Ignition Devolatilization' model (UID model, herein) is developed which is evolved based on the diffusion-limited classical droplet theory (for more details refer [19]). In this paper, the particle is ignited by incorporating a convective external heat flux and the devolatilization phase is computed by applying the thin film boundary condition from the application of droplet combustion theory as explained in [25]. The particle is assumed to be perfectly insulated from the sides and bottom and hence, the particle receives heat only from one direction (top layer). As the one layer of dry timber particle surface gets heated up to a critical temperature, called the pyrolysis temperature, volatiles are released from the particle from which the flame envelopes the particle and burns in gas phase. In the model, there are four distinct zones as shown in Fig. 2.

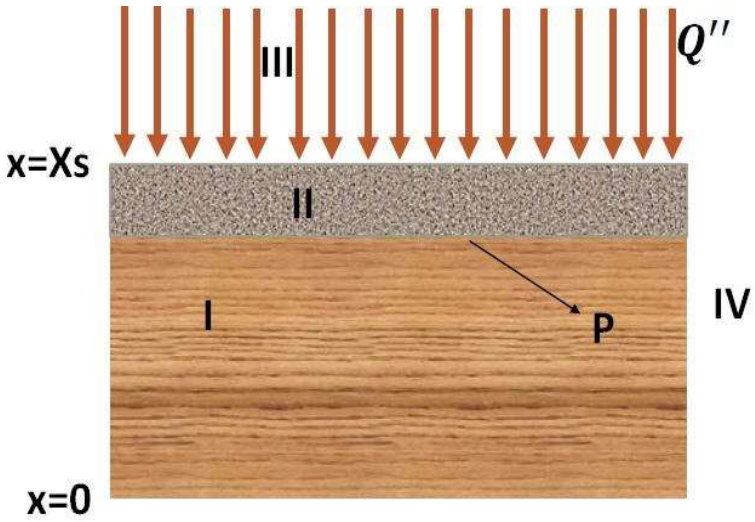

Fig. 2 Basic Elements of the current model

Region I: Virgin wood; Region II: Charred area; Region III: gas phase between the particle and flame; Region IV: Ambient zone

P indicates the propagating pyrolysis front, and Q" is the incident heat flux. The thin zone is the pyrolysis front at the pyrolysis temperature. The particle's progression, when exposed to high temperatures, species, and energy conservation equations are used for all four regions. Region 1 is subjugated by transient conduction, whereas the other zones are taken to be quasi-steady-states [19]. This assumption is valid as the pyrolysis movement rate is minimal compared to gas velocities. The governing equations for single-particle combustion are given in (1) - (3)

Region 1: $(0 \leq x \leq x_p(t))$

$$\frac{\partial T}{\partial t} = \alpha \frac{\partial^2 T}{\partial x^2} \tag{1}$$

Region 2: $(x_p(t) \leq x \leq \infty)$

$$G_p c_p \frac{\partial T}{\partial x} = k \frac{\partial^2 T}{\partial x^2} \tag{2}$$

$$G_p c_p \frac{\partial Y_i}{\partial x} = k \frac{\partial^2 Y_i}{\partial x^2} \tag{3}$$

The interface and boundary conditions for the above are given in (4) – (8)

$$-k \frac{\partial T}{\partial x}|_{x_s} = Q''(x_s, t) \;\; \& \;\; -k \frac{\partial T}{\partial x}|_{x_s^+}^{x_s^-} + Q'' = \sigma \in T_s^4 \tag{4}$$

$$T(x,0) = T_\infty \quad \& \quad T(\infty,t) = T_\infty \tag{5}$$

$$Y_{ox}(\infty,t) = Y_{ox,\infty} \quad \& \quad T(\infty,t) = T_\infty \tag{6}$$

$$-k\frac{\partial T}{\partial x}|_{x_p^+}^{x_p^-} = G_p H_d \quad \& \quad k\frac{\partial T}{\partial x}|_{x_p^-} = q_w'' \tag{7}$$

$$\rho D\frac{\partial Y_f}{\partial x}|_{x_f^-}^{x_f^+} = \rho D\frac{\partial Y_o}{\partial x}|_{x_f^-}^{x_f^+}/s \quad \& \quad k\frac{\partial T}{\partial x}|_{x_f^-}^{x_f^+} = \rho D H_C Y_f|_{x_f^-}^{x_f^+} \tag{8}$$

3.1 Timber Ignition

A timber particle is considered ignited if a stable diffusion flame is formed around, it when exposed to an ignition source. A quasi-1-D method outlined in [19] is used. Fresh timber of thickness ($x_{s)}$ at ambient temperature when suddenly exposed to a heat source, its the surface temperature (T_s) starts to increase. This heating up time can be computed by solving a transient heat conduction equation subjected to heat flux q_w''. Once the surface reaches the pyrolysis temperature (T_p), it starts releasing 'volatiles' and now the pyrolysis front (x_p) regresses towards the bottom. Assuming that the chemical reactions are confined to the thin pyrolysis front, mass conservation; implies that the mass flow rate at any thickness is constant, i.e., $G = G_p = G_s$ where, G_p is mass flux in kg/m^{2}s at the pyrolysis front.

Region 2: $(X_p(t) \leq x \leq \infty)$

Integrating (2) and using $G = G_p = G_s$ yields

$$GC_pT - k\frac{dT}{dx} = G_pC_pT_P - k\frac{dT}{dx}|_{x_p^+} \tag{9}$$

Since the temperature profile in the virgin wood particle is determined entirely with the boundary conditions specified, $k\frac{\partial T}{\partial x}|_{x_p^-}$ Can be evaluated. Let this be q_w''. Now expressing $\frac{\partial T}{\partial x}|_{x_p^+}$ in terms of q_w'' using (7) yields

$$G_pC_pT - k\frac{dT}{dx} = G_pC_pT_p - \left(q_w'' + G_pH_d\right) \tag{10}$$

$$G_pC_p\left[T - T_p + \frac{H_d}{c_p} + \frac{q_w''}{G_pc_p}\right] = k\frac{dT}{dx} \tag{11}$$

Integrating again gives

$$ln\left\{\frac{T_p - T_p + \frac{H_d}{c_p} + \frac{q_w''}{G_pc_p}}{T - T_p + \frac{H_d}{c_p} + \frac{q_w''}{G_pc_p}}\right\} = \frac{G_pc_p}{k}\left[x_p - x\right] \tag{12}$$

Substituting $T = T_s$ @ $x = x_s$

$$ln\left\{\frac{\frac{H_d}{c_p} + \frac{q_w''}{G_pc_p}}{T_s - T_p + \frac{H_d}{c_p} + \frac{q_w''}{G_pc_p}}\right\} = \frac{G_pc_p}{k}\left[x_p - x_s\right] \tag{13}$$

where

G_p is the mass flux at pyrolysis front (x_p)

T_s, T_p are the temperature at the surface and pyrolysis front

c_p is the specific heat capacity at constant pressure

k is the thermal conductivity

q_w'' is heat flux into fresh biomass

H_d is the heat of decomposition of volatiles

3.2 Timber devolatilization

In the current approach, the ignition to devolatilization switch, is attained by replacing the convective boundary condition to a thin flame boundary condition as given in [19,25]. As the flame engulfs the particle,

the surface receives heat from the flame, and the particle surface radiation effects becomes dominant. To determine the heat transferred to the surface, temperature profile from the flame to surface has to be evaluated. In order to do the same, a conserved scalar approach is adopted and after incorporating necessary boundary conditions, Eq.(24) was arrived at.

From $X_p(t) \leq x \leq \infty$:

$$GC_pT - k\frac{dT}{dx} = -\dot{\omega}_f'''H_C \tag{14}$$

$$Gc_pY_{ox} - \rho D\frac{dY_{ox}}{dx} = s\dot{\omega}_f''' \tag{15}$$

H_C is the heat of combustion of volatiles, and s is the stoichiometric ratio. For Le=1, we eliminated the source terms on the right-hand side.

$$G\phi - \frac{k}{c_p}\frac{d\phi}{dx} = 0 \tag{16}$$

where ϕ is the conserved scalar given by $c_pT + \frac{H_cY_{ox}}{s}$. Integrating the above equation gives

$$G_p\phi - \frac{k}{c_p}\frac{d\phi}{dx} = G_p\phi_s - \frac{k}{c_p}\frac{d\phi}{dx}|_{x_s^+} \tag{17}$$

Integrate the above equation again,

$$ln\left[\frac{\phi-\phi_s+\frac{k}{G_pc_p}\frac{d\phi}{dx}|_{x_s^+}}{\phi_\infty-\phi_s+\frac{k}{G_pc_p}\frac{d\phi}{dx}|_{x_s^+}}\right] = \frac{G_pc_p}{k}[x] \tag{18}$$

Substitute ϕ=ϕ_s @ x=x_s and rearrange the above equation to get $\frac{d\phi}{dx}|_{x_s^+}$

$$\frac{d\phi}{dx}|_{x_s^+} = \frac{G_pC_p(\phi_\infty-\phi_s)}{k\left[expexp\left(-\frac{G_pC_px_s}{k}\right)-1\right]} \tag{19}$$

Evaluate ϕ at x_s and ∞

$$\phi_s = c_pT_s + \frac{H_cY_{ox,s}}{s} = c_pT_s \tag{20}$$

$$\phi_\infty = c_pT_\infty + \frac{H_cY_{ox,\infty}}{s} \tag{21}$$

By differentiating ϕ w.r.t x at x=x_s^+ we get

$$\frac{d\phi}{dx}|_{x_s^+} = c_p\frac{dT}{dx}|_{x_s^+} \tag{22}$$

Equating 19 and 22 and substitute 20 and 21, we get

$$k\frac{dT}{dx}|_{x_s^+} = G_p\left[\frac{C_p(T_\infty-T_s)+\frac{H_cY_{ox,\infty}}{s}}{expexp\left(-\frac{G_pc_pX_s}{k}\right)-1}\right] \tag{23}$$

Using 11 and 23 in 4 yields

$$G_p\left[\frac{C_p(T_\infty-T_s)+\frac{H_cY_{ox,\infty}}{s}}{expexp\left(-\frac{G_pc_pX_s}{k}\right)-1}Nu - c_p\left(T_s-T_p\right) - H_d - \frac{q_\omega''}{G_p}\right] + Q'' = \sigma \in T_s^4 \tag{24}$$

where

$Y_{ox,\infty}$ is the free stream mass fraction of O_2, i.e., 0.232

T_∞ is the ambient temperature

σ is the Stefan-Boltzmann constant

$\in$ is the emissivity at the surface.

Here, the pyrolysis temperature of 473 K is assumed which is the critical temperature around which the volatiles are released which is in the range that is applicable to most of the biomass including CLT. It is important to mention here that, even if the pyrolysis temperature is varied it has no effect in predicting the burning behaviour of the particle except for a slight shift in ignition time. Also, the flame propagation is governed by heat transfer, the model could predict the mass loss rate (MLR herein) more accurately rather than cumbersome kinetic models which was the approach used to solve these problems by earlier researchers. More discussions on diffusion limitedness of the biomass, subjective to similar boundary conditions are discussed in details in our earlier works [19,23,26]. The thermos-physical properties used in the model for the timber particle is listed in Table 2.

Table 2. Thermo-physical properties of Radiata pine timber [17,18,25].

S No	Description	Values	Units
1.	Mass of the sample	524.4	g
2.	Density of sample	436.98	Kg/m^3
3.	Thermal conductivity of the sample	0.308	W/mK
4.	Specific heat capacity	1200	J/kg k
5.	Thermal diffusivity	5.874 x 10^{-7}	m^2/s
6.	Enthalpy of combustion of volatiles	16	MJ/kg
7.	The heat of decomposition of volatiles	180	kJ/kg

3.3 Char Oxidation

In addition to the external heat flux received at the particle surface and heat radiated from the flame, there is an additional heat flux which is present in this case which is due to char oxidation. As the burning takes place with excess air mode, char oxidation is one another parameter which influences the burning rate of the timber particle and should be considered in the model as explained below.

The heat balance at the receding surface is given by

$$\rho_{char} c_{pchar} \dot{r} (T_{si} - T_c) = q_s'' \quad (25)$$

where

$\dot{r}$ is the surface regression rate

T_{si} is the temperature at the reaction surface

T_c is the core temperature

q_s'' heat generated from the surface reaction.

ρ_{char}, c_{pchar}, T_{si}, T_c values are taken from [9]. $\dot{r}$ is given by

$$\dot{r} = G_p / \rho \quad (26)$$

Final governing equations including char oxidation effect are given by

$$ln \left\{ \frac{\frac{H_d}{c_p} + \frac{q_w''}{G_p c_p} + \frac{q_s''}{G_p c_p}}{T_s - T_p + \frac{H_d}{c_p} + \frac{q_w''}{G_p c_p} + \frac{q_s''}{G_p c_p}} \right\} = \frac{G_p c_p}{k} \left[X_p - X_s \right] \quad (27)$$

$$G_p\left[\frac{\frac{C_p(T_\infty - T_s)+\frac{H_c Y_{ox,\infty}}{s}}{expexp\left(-\frac{G_p c_p X_s}{k}\right)-1}Nu - C_p(T_s - T_p) - H_d - \frac{q_w''}{G_p} - \frac{q_s''}{G_p}\right] + Q'' - q_s'' = \sigma \in T_s^4 \quad (28)$$

4 RESULTS AND DISCUSSIONS

Matlab® is used to solve the transient conduction equation and to get the heat flux into the fresh timber and ignition temperature profile. After ignition, switch over to the thin flame boundary condition takes place. Then equations (27) and (28) are simultaneously solved for G_p and T_s using the value of heat flux q_w'' computed from the transient conduction solver. The iteration continues for one hour which is the typical experimental duration as mentioned in [18]. The initial incident heat flux is given as 50 kW/m^2 for the duration of 1200 seconds after which the particle attains the steady state. After 1200 seconds, the heat flux is changed to see the effect of the same over extinction of the particle. The MLR is calculated using the following formula.

$$MLR = \frac{[(G_p \times dt \times Y_{fpm})]}{t} \quad (29)$$

A graph between MLR and time is plotted as shown in Fig. 3 and Fig. 4 for the cases as mentioned in Table1.

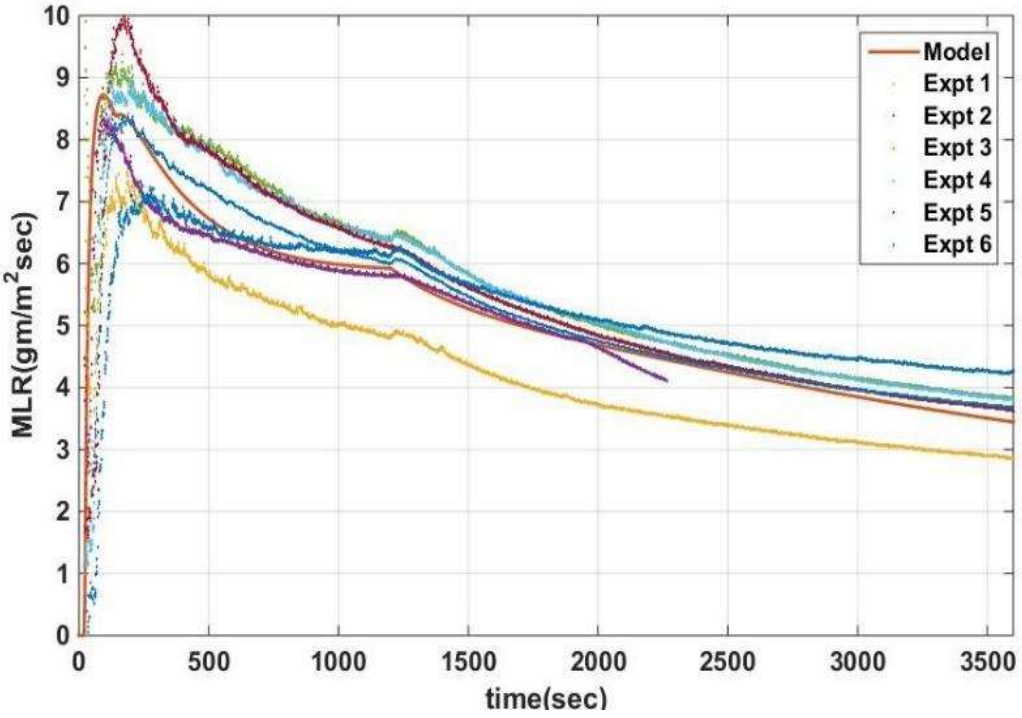

Figure 3. MLR vs. time for 30 kW/m^2 heat flux

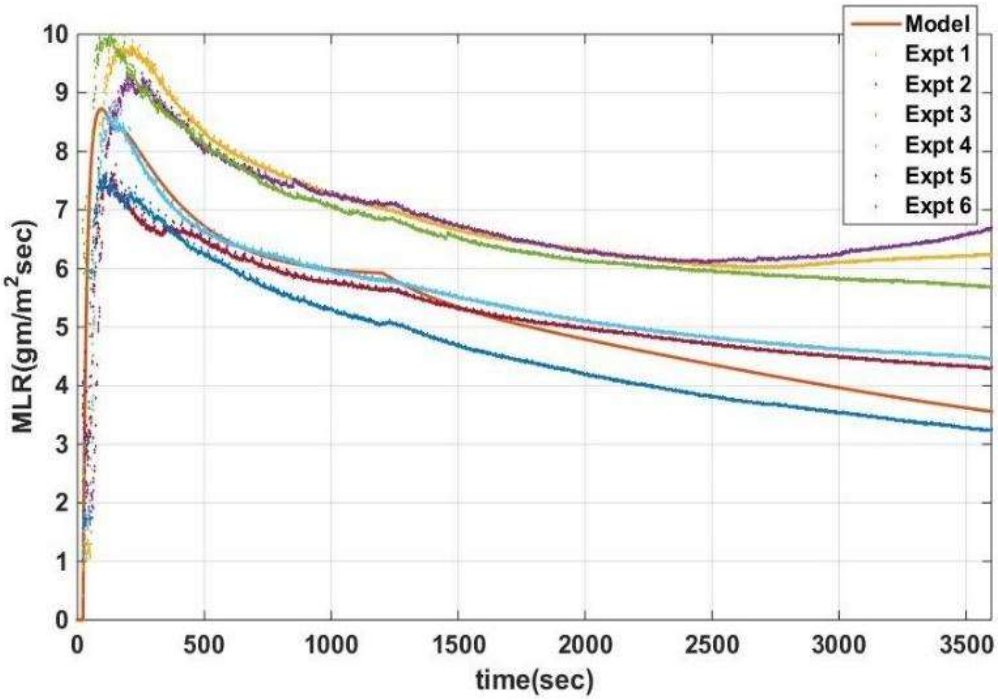

Figure 4. MLR vs. time for 40 kW/m^2 heat flux

It is very clear from the plot of MLR versus time for both the air cases that, the model predictability is very good and lies within the experimental limits. As seen from Fig. 3 and fig. 4, there is a rate of MLR decline is similar for both 30 kW/m^2 and 40 kW/m^2 cases. However, as for the same time frame the rate of MLR decline of 30 kW/m^2 case is more than 40 kW/m^2 case. In other words, when time elapses, the accumulation of char layer increases which decreases heat transport to the fresh layer of biomass which hinders the devolatilization process and there is a decrease in MLR. This is less pronounced when there is an additional heat flux of 40 kW/m^2 which enhances the MLR and it is above 4 g/m^{2}s at 3000 seconds but it drops to less than 4 g/m^{2}s for 30 kW/m^2 case around the same time frame. Hence, accounting for the experimental uncertainties, the criteria of self-extinction for timber can be set as less than 4 g/m^{2}s when the time of burning reaches near 85% of the total time i.e. 3000 seconds. The same phenomenon is expected with decreased oxygen fraction cases too. But, the accumulation rate of char layer can be higher for low oxygen fractions and this in authors opinion, needs further validation to firmly conclude the boundary limits of self-extinction in such operating regimes. This will be taken up later.

5 CONCLUSIONS

In this present work, a transient one dimensional mathematical model has been developed to predict the flame extinction and burning behaviour of the radiata pine timber. The mass loss rate (MLR) predictions for the air cases with different heat flux cases is agreeing well with the experimental data which proves the model capability to capture the underlying phenomenon of timber burning. When the MLR drops below 4 g/m^{2}s, it can be termed as extinction of the flame and this is point where the resistance of heat flow to the surface of the fresh layer predominates the heat diffusion for further devolatilization. However, with decreased oxygen fractions, this criterion needs further validation and this will be pursued in future.

REFERENCES

1. A. Tewarson, R.F. Pion, Flammability of plastics-I. Burning intensity, Combust. Flame. 26 (1976) 85–103. doi:10.1016/0010-2180(76)90059-6.
2. R. V. Petrella, The mass burning rate and mass transfer number of selected polymers, wood, and organic liquids, Polym. Plast. Technol. Eng. 13 (1979) 83–103. doi:10.1080/03602557908067676.
3. R. Emberley, A. Inghelbrecht, Z. Yu, J.L. Torero, Self-extinction of timber, Proc. Combust. Inst. 36 (2017) 3055–3062. doi:10.1016/j.proci.2016.07.077.
4. R. Emberley, T. Do, J. Yim, J.L. Torero, Critical heat flux and mass loss rate for extinction of flaming combustion of timber, Fire Saf. J. 91 (2017) 252–258. doi:10.1016/j.firesaf.2017.03.008.
5. R. Crielaard, J.W. van de Kuilen, K. Terwel, G. Ravenshorst, P. Steenbakkers, Self-extinguishment of cross-laminated timber, Fire Saf. J. 105 (2019) 244–260. doi:10.1016/j.firesaf.2019.01.008.
6. A. Bartlett, R. Hadden, L. Bisby, B. Lane, Auto-extinction of engineered timber: the application of firepoint theory, Interflam. (2016).
7. T.J. Ohlemiller, T. Kashiwagi, K. Werner, Wood gasification at fire level heat fluxes, Combust. flame. 69 (1987) 155–170. doi:10.1016/0010-2180(87)90028-9.
8. P. Reszka, J.L. Torero, In-depth temperature measurements in wood exposed to intense radiant energy, Exp. Therm. Fluid Sci. 32 (2008) 1405–1411. 506 doi: 10.1016/j.expthermflusci.2007.11.014.
9. TJ Ohlemiller, T Kashiwagi, and K Werner. Wood gasification at fire level heat fluxes. Combustion and Flame, 69(2):155–170, 1987.
10. T Kashiwagi, TJ Ohlemiller, and K Werner. Effects of external radiant flux and ambient oxygen concentration on nonflaming gasification rates and evolved products of white pine. Combustion and Flame, 69(3):331–345, 1987.
11. Esko Mikkola. Charring of wood based materials. Fire Safety Science, 3:547–556, 1991.
12. Michael A Delichatsios. Piloted ignition times, critical heat fluxes and mass loss rates at reduced oxygen atmospheres. Fire Safety Journal, 40(3):197–212, 2005.
13. Vytenis Babrauskas. Charring rate of wood as a tool for fire investigations. Fire Safety Journal, 40(6):528–554, 2005.
14. Yibing Xin and Mohammed M Khan. Flammability of combustible materials in reduced oxygen environment. Fire safety journal, 42(8):536–547, 2007.
15. Chris Lautenberger and Carlos Fernandez-Pello. A model for the oxidative pyrolysis of wood. Combustion and Flame, 156(8):1503–1513, 2009.
16. David Barber and Robert Gerard. Summary of the fire protection foundation report-fire safety challenges of tall wood buildings. Fire Science Reviews, 4(1):1–15, 2015.
17. Ariel R D´ıaz, Erick I Saavedra Flores, Sergio J Yanez, Diego A Vasco, Juan C Pina, and Carlos F Guzm´an. Multiscale modeling of the thermal conductivity of wood and its application to cross-laminated timber. International Journal of Thermal Sciences, 144:79–92, 2019.
18. Juan Cuevas, Jose Luis Torero, and Cristian Maluk. Flame extinction and burning behaviour of timber under varied oxygen concentrations. Fire Safety Journal, page 103087, 2020.
19. Jaganathan VM, Kalyani AM & Varunkumar S (2017). “Unified ignition-devolatalization model for fixed bed biomass gasification/combustion, Jaganathan VM, Kalyani AM & Varunkumar S (2019). Energy Procedia, Volume 120, 643-648. INFUB-11, Portugal.
20. VM Jaganathan. Syngas synthesis using gasification of biomass with O_2–CO_2 and O_2–steam mixtures. PhD diss., Indian Institute of Technology, Madras, 2019.
21. Jaganathan VM, Omex Mohan & Varunkumar S (2019). “Intrinsic hydrogen yield from gasification of biomass with oxy-steam mixtures ”. International Journal of Hydrogen Energy, Volume 44, 17781-17791.
22. Jaganathan VM, & Varunkumar S (2019). “Net carbon-di-oxide conversion and other novel features of packed bed biomass gasification with O2/CO2 mixtures ”. Fuel, Volume 244, 545-558.
23. Kalyani AM, Jaganathan VM & Varunkumar S (2019). Mechanisms governing the 'gasification to char oxidation transition' in counter-current flame propagation in packed beds: insights from single particle experiments, Particle Science and Technology, Volume 39, 490-494, doi: 10.1080/02726351.2020.1767245.
24. R. Emberley, A. Inghelbrecht, Z. Yu, J.L. Torero, Self-extinction of timber, Proc. Combust. Inst. 36 (2017) 3055–3062. doi:10.1016/j.proci.2016.07.077.

25. HS Mukunda, PJ Paul, U Srinivasa, and NKS Rajan. Combustion of wooden spheres-experiments and model analysis. In Twentieth Symposium (International) on Combustion/The Combustion Institute, pages 1619–1628. Twentieth Symposium (International) on Combustion/The Combustion Institute, 1984.
26. S Varunkumar. Packed bed gasification-combustion in biomass based domestic stoves and combustion systems. Indian Institute of Science, 2012.